Supercond. Sci. Technol. 7 (1994) 277–280. Printed in the UK

Investigation of $SrRuO_3$ barriers in SNS junctions

R Dömel†, C L Jia‡, C Copetti†, G Ockenfuss† and A I Braginski†

† Institut für Schicht- und Ionentechnik (ISI), Forschungszentrum Jülich (KFA), 52425 Jülich, Germany

‡ Institut für Festkörperforschung, Forschungszentrum Jülich (KFA), 52425 Jülich, Germany

Received 7 December 1993

Abstract. High-quality films and multilayers of $SrRuO_3$ and $YBa_2Cu_3O_7$ (YBCO) have been grown by off-axis sputtering. High-resolution transmission electron microscopy proved that the interface is atomically sharp. SNS junctions with $SrRuO_3$ barriers have been fabricated *ex situ* in an edge geometry, and in a sandwich geometry with both interfaces grown *in situ*. Supercurrents have been observed with barrier thicknesses from 10 to 40 nm, and Shapiro steps could be detected. In both junction geometries the normal resistance is several orders of magnitude higher, as would be expected from the resistance of the SrRuO film, and shows a non-metallic temperature dependence. An exponential dependence of the normal resistance upon the barrier thickness has been observed.

1. Introduction

Metallic perovskites are a promising alternative to noble metal barrier materials in SNS junctions. Their epitaxial growth, for example on $YBa_2Cu_3O_7$, makes sandwich and edge geometries possible. Also, it can be expected that the S–N mismatch of the Fermi velocities is not as large as for silver or gold. The perovskite system $(Sr_{1-x}Ca_x)RuO_3$ has been investigated by Char and co-workers [1, 2]. Single crystals of the tetragonal Sr_2RuO_4 have been grown by Lichtenberg *et al* [3], but thin films of this phase are difficult to grow because the much more stable $SrRuO_3$ phase is formed. SNS junctions with ferromagnetic $SrRuO_3$ have been investigated by Antognazza *et al* [2]. In that work, supercurrents were observed up to a thickness of 25 nm and the junction resistance was determined by the SN interface, similar to SNS junctions with noble metal barriers [4]. In our work, junctions with *in situ* and *ex situ* interfaces have been investigated to distinguish between extrinsic effects due to damage in the patterning process and those due to a mismatch of the lattice constants, thermal expansion coefficients or of Fermi velocities. Furthermore, a detailed study of multilayers and the SN interface has been done by means of high-resolution transmission electron microscopy.

2. Film growth

Epitaxial films of $SrRuO_3$ were grown by off-axis sputtering on $SrTiO_3$ and $LaAlO_3$ substrates. The x-ray patterns indicated a cubic material with a lattice constant of 3.97 Å. Rocking-curve widths of 0.05° and Rutherford backscattering channelling minimum yields of 3% proved an excellent crystalline quality. The temperature dependence of the electric conductivity was metallic with a cusp at 150 K due to a decrease in the spin-flip scattering, as reported in [2, 5]. The specific resistance of the films was 8×10^{-4} Ω cm at 300 K, about two orders of magnitude higher than that of Au or Ag. The superconducting properties of YBCO *c*-axis films grown on $SrRuO_3$ were similar to those on the usual epitaxial substrate materials. A minimum channelling yield of 4% has been observed.

Figure 1 shows a transmission electron microscope (TEM) picture of the interface between $SrRuO_3$ and YBCO. The interface is atomically sharp but exhibits many steps. Numerical simulations of the interface atoms show that there is no interdiffusion. The TEM results have been reported in more detail by Jia *et al* [6].

A serious problem for the growth of multilayers is that the high-quality $SrRuO_3$ film allows no diffusion of oxygen at the usual oxygenating temperatures of YBCO, i.e. between 400 and 500 °C. The result is that, after the usual film annealing procedure of a trilayer, the lower YBCO film is always oxygen depleted. Figure 2 shows the θ–2θ scan of a trilayer of YBCO with a 10 nm $SrRuO_3$ interlayer. In figure 2(*a*), the YBCO (005) reflex consists of two peaks, which belong to a superconducting top YBCO layer with a *c* axis of $c = 11.6$ Å and an oxygen-deficient bottom layer with $c = 11.8$ Å. A special oxygenating procedure at temperatures between 680 and 720 °C is needed to cause oxygen diffusion. Figure 2(*b*) shows the (005) reflex of the trilayer

0953-2048/94/050277 + 004 $19.50

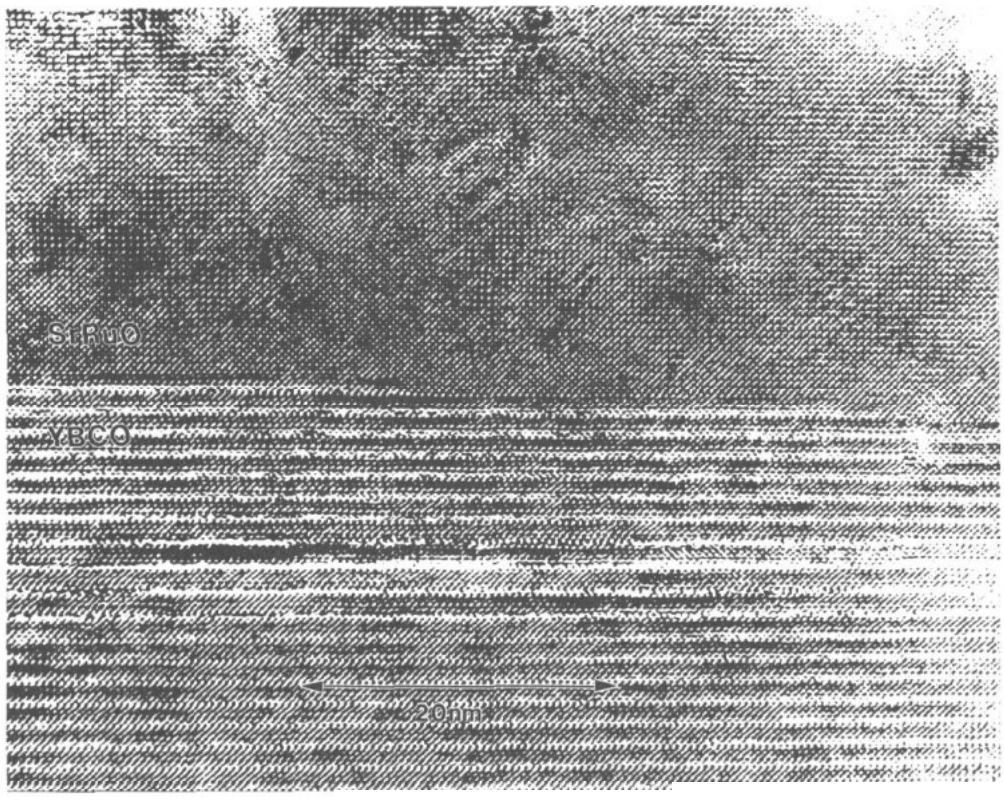

Figure 1. High-resolution lattice image of the interface between YBCO and $SrRuO_3$ taken along the [100] direction of YBCO.

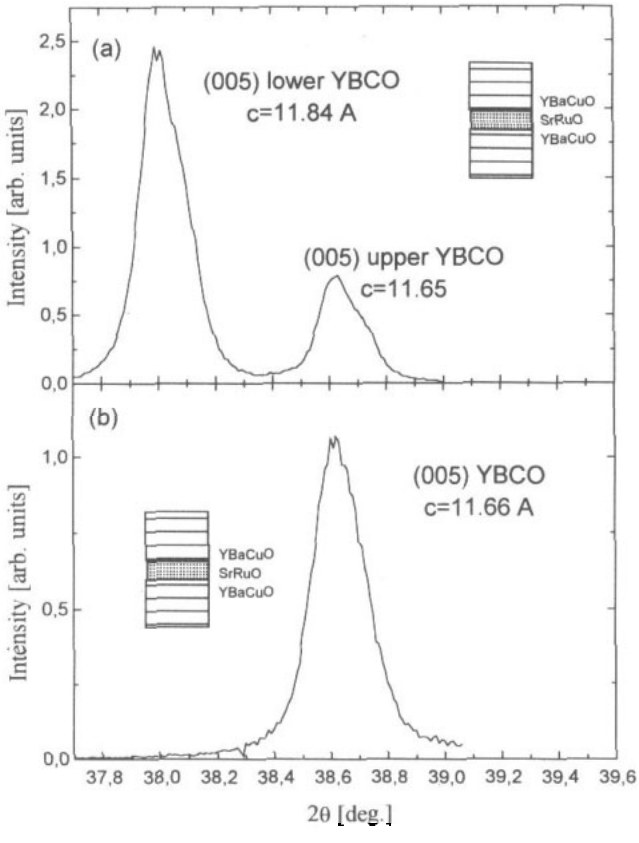

Figure 2. θ–2θ scan of a trilayer with a 10 nm thick $SrRuO_3$ barrier; the lower layer is about 90 nm, the upper layer about 50 nm. (*a*) After the usual oxygenating procedure the lower film is oxygen depleted; (*b*) after 1–2 h at 680 °C both films are fully oxygenated.

after 1 h annealing in 1 atm oxygen at 680 °C, which indicates that both layers are properly oxygenated.

The fact that no oxygen diffuses even through an $SrRuO_3$ film only 10 nm thick shows that the barrier is perfectly grown.

3. Fabrication and measurements of SNS junctions

Two different types of junctions have been fabricated. The first fabrication approach involved an edge junction, where the YBCO edge was etched by non-aqueous Br–ethanol solution, using the method developed by Faley *et al* [7]. Figure 3 shows a scheme of the patterning process. The bottom YBCO film is etched through a mask of CaO and ZrO, which is patterned by a usual resist lift-off process. The mask stays on the bottom layer during the *in situ* deposition of the $SrRuO_3$ barrier and the top YBCO layer and is finally lifted-off in water (see Roas [8]) to remove the *c*-axis shunt. In the last step, bridges of 2 to 20 μm width are patterned by ion beam etching (IBE).

The current–voltage (I–V) characteristic of this type of junction with a nominal barrier thickness of 30 nm and a bridge width of 5 μm is shown in figure 4. The critical current I_c was 400 μA and the normal resistance $R_N = 18\ \Omega$ at 4.2 K ($I_c R_N = 7.2$ mV), determined by suppressing the supercurrent by microwave irradiation.

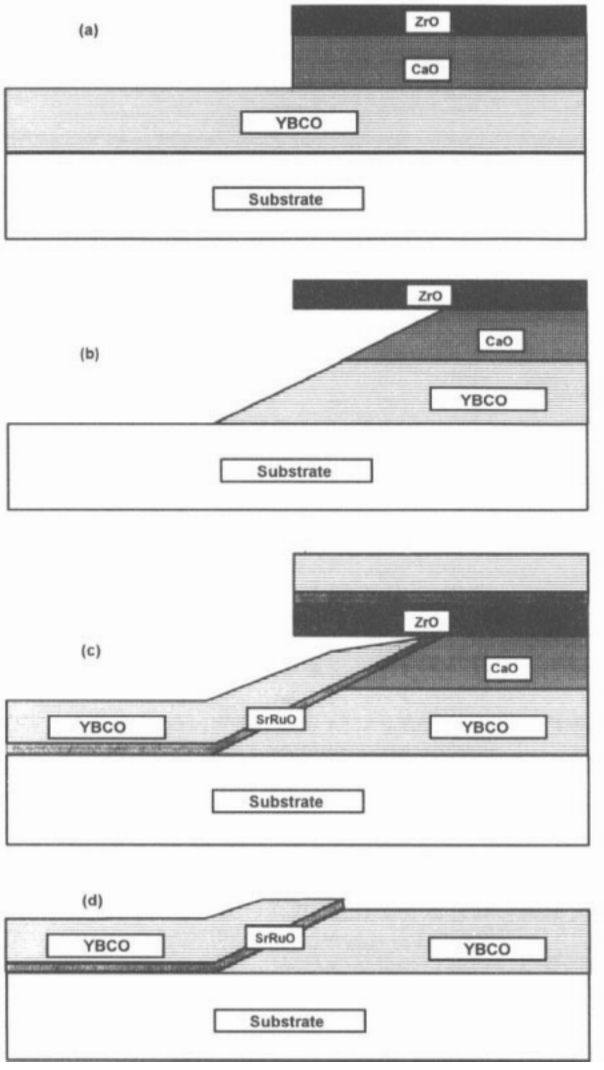

Figure 3. Fabrication of the edge-type junction: (*a*) a mask of CaO and ZrO is patterned by lift-off, (*b*) YBCO is etched by 0.3% Br in ethanol, (*c*) the $SrRuO_3$ barrier and top YBCO layer are deposited, (*d*) CaO and the top layers are lifted off in H_2O.

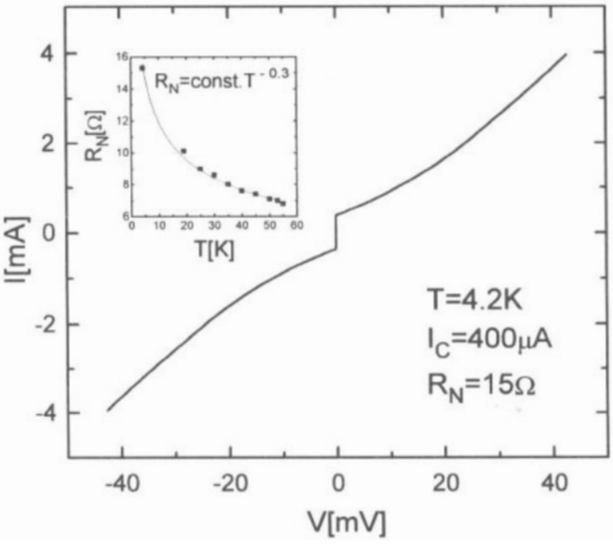

Figure 4. *I–V* curve of an *ex situ*-type junction: junction width 5 μm, barrier thickness 30 nm.

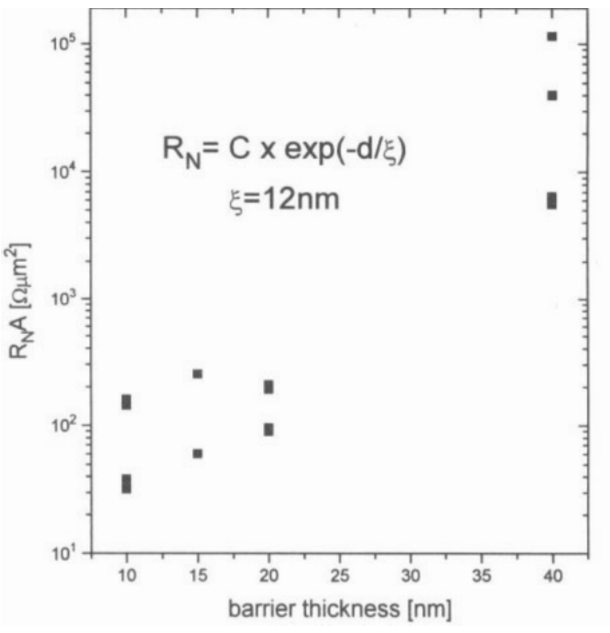

Figure 5. Thickness dependence of the normal resistance of the *in situ* junctions multiplied by the junction area.

Supercurrents have been observed up to 55 K. The R_N was three orders of magnitude higher (R_N × junction area/barrier thickness $\simeq 0.1\ \Omega$ cm) than expected from the film resistivity ($\rho \simeq 10^{-4}\ \Omega$ cm) and, as can be seen from the inset in figure 4, the temperature dependence was not metallic. The data for a barrier thickness of 30 nm can be approximated by the expression $R \propto \exp(T^{-0.3})$, which suggests two-dimensional variable-range hopping as a possible transport mechanism for the normal current [9].

To prepare junctions with both *in situ* interfaces, a *c*-axis-oriented trilayer of YBCO/$SrRuO_3$/YBCO was fabricated and junction areas of 2 μm × (2 μm–20 μm) × 20 μm were patterned by ion beam etching. The base electrode and the sidewalls were insulated by MgO and the upper electrode was contacted by gold leads, which allows a three-point measurement of the SNS junctions. Junctions with barrier thicknesses from 10 to 40 nm were fabricated and showed supercurrents. The observation of supercurrent in this *c*-axis geometry may be due to the atomic steps at the interface (see figure 1) which allow the flow of supercurrents along the *a–b* planes. On the other hand, supercurrents along the YBCO *c* axis through ferromagnetic barrier materials have also been observed by Kasai *et al* [10]. The critical current of our junctions at 4.2 K varied from 5 μA to 800 μA at 4.2 K, depending on the junction area and the barrier thickness. Shapiro steps have been observed above 40 K. The normal resistance of these junctions was as high as in the edge junction geometry, and increased nearly linearly with temperature.

The critical current density for a given junction area varied by about one order of magnitude. Therefore, the I_c data were not reliable enough to determine a dependence on the barrier thickness. However, the normal

resistance of the junctions was much more reproducible and increased exponentially with the barrier thickness. The data could be fitted by $R_N \sim \exp(-d/\xi_n)$, with a characteristic length ξ_n of 12 ± 4 nm (see figure 5).

3. Discussion

That the normal resistance of the junctions is several orders of magnitude higher than would be expected from the resistance of the $SrRuO_3$ films has already been reported by Char and co-workers [2, 11] and explained by the resistance of the SN interface, which is independent of the barrier thickness. In our case the junction resistance is not determined by the interface only, since we see an exponential dependence of R_N on the barrier thickness. Furthermore, the comparison between the two types of junctions shows that the non-metallic temperature dependence is independent of geometry and interface quality. The critical current shows no significant thickness dependence, which suggests a different transport mechanism for Cooper pairs and the normal current, but may also be explained by a random number density of atomic steps at SN interfaces. It is not yet clear if there are any pair-breaking effects due to the ferromagnetic $SrRuO_3$ barrier. Antognazza *et al* [2] reported that above a thickness of 25 nm no critical currents could pass the barrier. In our case, the junctions with the thickness barrier (40 nm) showed supercurrents of about 10 μA at 4.2 K. A possible explanation could be fluctuations of the barrier thickness, which allow supercurrents only in the area where the barrier is thinner than the critical thickness. However, while TEM investigations give only a local picture, they show that the barrier thickness varies only within a few nanometres and is determined by the roughness of the lower YBCO layer and the presence of atomic steps.

Acknowledgments

We would like to thank M Siegel for helpful discussions and Y Xu and S S Ata-Allah for the preparation of the sputtering targets. This work was supported, in part, by the BMFT Consortium 'First Applications of HTS in Micro- and Cryoelectronics', project Nos 13N5811 and 13N5812.

References

[1] Char K, Colclough S, Geballe T H and Myers K E 1993 *Appl. Phys. Lett.* **62** 197
[2] Antognazza L, Char K and Geballe T H 1993 *Appl. Phys. Lett.* **63** 7
[3] Lichtenberg F, Catana A, Mannhart J and Schlom D G 1992 *Appl. Phys. Lett.* **60** 9
[4] Ono R H, Beall J A, Cromar M W, Harwey T E, Johansson M E, Reintsema C D and Rudman D A 1991 *Appl. Phys. Lett.* **59** 9
[5] Wu X D, Foltyn S R, Dye R C, Coulter Y and Muenchausen R E 1993 *Appl. Phys. Lett.* **62** 19
[6] Jia C L, Dömel R and Urban K 1994 *Phil. Mag. Lett.* submitted
[7] Faley M I, Poppe U, Soltner H, Jia C L, Siegel M and Urban K 1993 *Appl. Phys. Lett.* **63** 15
[8] Roas B 1991 *Appl. Phys. Lett.* **59** 20
[9] Mott N F and Davis E A 1979 *Electronic Properties of Doped Semiconductors* (Oxford: Clarendon)
[10] Kasai M, Kanke Y, Ohno T and Kozono Y 1992 *Appl. Phys.* **72** 11
[11] Char K, Antognazza L and Geballe T H 1993 *Appl. Phys. Lett.* **63** 17